Tissue and Cell 93 (2025) 102769

Contents lists available at ScienceDirect

Tissue and Cell

journal homepage: www.elsevier.com/locate/tice

Macro- and microscopic morphology of the rectal gland of the Brazilian guitarfish (*Pseudobatos horkelii*) from Southeastern Brazil

Beatriz França Lopes [a,1], Géssica Vieira Gomes [b,2], Hassan Jerdy [c,3], Rachel Ann Hauser-Davis [d,*,4], Eulógio Carlos Queiroz de Carvalho [e,*,5]

[a] *Animal Morphology and Pathology Laboratory, Center for Agricultural Sciences and Technologies (CCTA)/Animal Pathology Sector (SPA), North Fluminense State University Darcy Ribeiro, Campos dos Goytacazes, RJ, Brazil*
[b] *Universidade Estadual Norte Fluminense Darcy Ribeiro, Campos dos Goytacazes, Rio de Janeiro, Brazil*
[c] *Laboratório de Microscopia, Universidade Federal do Sul e Sudeste do Pará, Rua Alberto Santos Dumont, Xinguara, PA, Brazil*
[d] *Laboratório de Avaliação e Promoção da Saúde Ambiental, Instituto Oswaldo Cruz, Fundação Oswaldo Cruz, Rio de Janeiro, RJ, Brazil*
[e] *CCTA/SPA, Campos dos Goytacazes, Rio de Janeiro, Brazil*

ARTICLE INFO

Keywords:
Salt gland
Rectal gland
Rays
Elasmobranchs
Histology
Pseudobatos

ABSTRACT

Sharks and rays present an osmoregulatory mechanism essentially exercised by a rectal salt gland. Histological assessments of this gland, however, are notoriously lacking. In this sense, histological assessments of the rectal gland of the Brazilian guitarfish, *Pseudobatos horkelii* obtained from off the coast of Rio de Janeiro, Brazil, were carried out herein. Rectal gland samples were histologically processed with hematoxylin/eosin and special Masson's Trichrome stain. Three main regions were identified: the capsule, secretory parenchyma and central duct. Highly vascularized connective tissue was observed in the capsular region, surrounded by a superficial epithelium composed of a layer of cubic cells. Lymphoid tissue was present outside the capsule. The capsule presented connective tissue invaginations, forming interlobular septa. Each septum, surrounded by fibroelastic tissue, delimited the secretory lobes filled with secretory tubules, whose lumens exhibited a larger diameter and a greater number of secretory cells as they approached the central duct. The duct to which the organ's secretory tubules open, at the center of the rectal gland, presents a lumen lined with stratified epithelium, containing acidophilic intraepithelial and mucous cells. Most analyzed morphological characteristics are in accordance with morphological aspects reported in previous ray studies concerning other species presenting similar phylogeny, habitat and feeding characteristics as *P. horkelii*. These assessments are paramount in understanding species-specific osmoregulation and informing conservation strategies, particularly for threatened species like the Brazilian guitarfish.

1. Introduction

Cartilaginous fishes belong to the *Chondrichthyes* class and are represented by two subclasses, *Holocephali* (comprising chimaeras) and *Elasmobranchii* (sharks and rays) (Chenhong et al., 2012; Amaral et al., 2017). The *Chondrichthyes* class is monophyletic, with all species presenting a superficially mineralized cartilaginous skeleton (Lund and Grogan, 1997).

Elasmobranchs are K-strategists, characterized by slow growth rates, late sexual maturity, low fecundity and long lifespans, resulting in low population increases and limited potential to recover from overfishing, chemical pollution and habitat destruction (Stevens et al., 2000). Given the cumulative impacts of fishing activities and low population growth rates, these animals are increasingly vulnerable to anthropogenic activities, although studies concerning their physiology and stress responses are still scarce.

* Corresponding authors.
E-mail addresses: rachel.hauser.davis@gmail.com (R.A. Hauser-Davis), eulogiocqcarvalho@gmail.com (E.C. Queiroz de Carvalho).
[1] 0009–0006-9759–4918
[2] 0000–0003-0341–8245
[3] 0000–0002-2373–2453
[4] 0000–0002-9451–471X
[5] 0000–0002-1785–8578

https://doi.org/10.1016/j.tice.2025.102769
Received 27 November 2024; Received in revised form 26 January 2025; Accepted 27 January 2025
Available online 29 January 2025

To maintain their internal homeostasis, elasmobranchs rely on ureo-osmoregulation, where urea synthesis occurs in the liver and accumulates in body fluids due to low gill permeability and active reabsorption by the kidneys (Boylan et al., 1967). As elasmobranch kidneys are incapable of producing urine more concentrated than blood plasma (Dantzler, 1989), these cartilaginous fishes display an extra-renal organ, the rectal gland, located in the caudal region, whose function of carrying out salt secretion, mainly sodium (Na) and chloride (Cl^-) ions, was discovered in the 1960s by Burger and Hess (1960). These ions are excreted in response to osmotic and volume changes in the internal elamsobranch environment. Specifically, when blood volume increases due to osmotic water influx in marine environments, the gland activates to expel excess salts, preventing hypernatremia and ensuring adequate osmotic balance, allowing elasmobranchs to maintain salt and fluid homeostasis in seawater, which is hyperosmotic to their body fluids (Solomon et al., 1984; Solomon et al., 1985; Erlij and Rubio, 1986). Because of this function, this organ is also termed the "rectal salt gland", as the secretory cells of this organ share characteristics with salt glands in reptiles and salt-secreting cells in birds (Doyle, 1962). The transport mechanism in the rectal gland epithelium involves chloride entering cells alongside Na and potassium (K) through a transporter located in the basolateral membrane, powered by the sodium electrochemical gradient maintained by Na^+K^+ATPase. Chloride exits the gland cells through a channel of the apical membrane, following an electrical gradient, while Na ions move into the rectal gland lumen down an electrical gradient through a paracellular pathway (Silva and Evans, 2024). For more details, please refer to a recent and comprehensive review on the subject, published by Silva and Evans (2024).

The unique contribution that the rectal gland offers to extrarenal osmo- and ionoregulation is related to its complex structure, responsible for secreting significant volumes of a hyperosmotic sodium chloride solution at about twice the plasma concentration (Forbush et al., 1992; Newbound and O'Shea, 2001). Several environmental contaminants, such as metals, have been noted as accumulating in this organ (Eyckmans et al., 2013; Wosnick et al., 2021), potentially leading to morphological changes and osmoregulation alterations. In this sense, a lack of information regarding rectal gland morphology in general is noted, even more so concerning rays, as this group is less studied than sharks, even though they are more endangered (Dulvy et al., 2021).

Guitarfish belong to the order Rhinopristiformes, within the subclass Elasmobranchii and the superorder Batoidea, allocated in the Rhinobatidae family. Phylogenetically, they used to be considered one of the more basal groups within Batoidea (McEachran and Carvalho, 1999; Nishida, 1990). However, a more recent study carried out in 2012 by Aschliman et al. examined the phylogenetic relationships among Batoidea skates and rays using molecular data and suggested that guitarfishes, traditionally grouped within the order Rhinopristiformes, do not form a monophyletic group. Instead, they appear to be paraphyletic, indicating that the evolution of body plans among these species is more complex than previously understood (Aschliman et al., 2012).

Guitarfish comprise about 35 species distributed across three genera: *Acroteriobatus*, *Rhinobatos*, and *Pseudobatos* (Fricke et al., 2024), the latter composed of *Pseudobatos horkelii* and *Pseudobatos percellens*, both of which occur in Brazil and are categorized as under threat according to the International Union for Conservation of Nature, with P. *percellens* listed as Endangered and P. *horkelii,* as Critically Endangered. These species are benthic, directly associated with sandy and muddy bottoms (McEachran and Carvalho, 1999) and abundant in deeper waters of up to 100 m (Martins and Schwingel, 2003). Guitarfish are caught as bycatch in various types of fisheries, particularly those targeting shrimp, employing beach seines and pair trawls (Leibold et al., 2004; Lessa et al., 1986; Vooren et al., 2005) in Brazil, and, due to heightened fisheries impacts, *P. horkelii* populations have declined by about 90 % off the southern Brazilian shelf from 1972 to 2002 (Vooren et al., 2005). Despite its highly endangered status and the increasing chemical contamination noted throughout this species habitat in southeastern Rio de Janeiro (Leite et al., 2023), studies concerning this species morpho-physiology are still notoriously lacking. In this context, this study aimed to investigate macroscopic and microscopic rectal gland features of this organ in the endangered Brazilian Guitarfish *Pseudobatos horkelii*.

2. Material and methods

The *Pseudobatos horkelii* individual analyzed herein, a male specimen, weighing and 1.825 kg and 82.0 cm in length, was captured by artisanal fishers in Copacabana, Metropolitan Region of the state of Rio de Janeiro, Southeastern Brazil, in April of 2021. Sampling was permitted by the Brazilian Chico Mendes Institute for Biodiversity Conservation, through SISBIO license no. 77310–5.

The specimen was dissected, and the rectal gland was removed and fixed in 10 % neutral buffered formalin for at least 48 hours. The tissue samples were then cleaved and processed on a Leica ASP300S tissue processor, dehydrated, clarified and paraffin impregnated for subsequent inclusion in paraffin blocks. Serial 5 μm-thick sections were prepared for routine staining with hematoxylin and eosin (HE) and special staining employing the Masson Trichrome stain. An optical Leica DM4B microscope (Leica microsystem CMS GmbH, Wetzlar, Germany) was utilized for microscopic analysis and photographic documentation,

3. Results

Located in the caudal region of the celomatic cavity, the rectal gland was observed to be connected to the post-valvular intestine, forming a blind-bottom sac situated between the colon and rectum. Its morphology resembled that of a pod, featuring a thin appendage with a lobed surface. Its blood supply is promoted by the posterior mesenteric artery, with drainage through the large dorsal intestinal vein. The structural distinctions between the secretory lobes, the central duct, and the venous vessel were more distinctly discernible in the transverse section, as depicted in Fig. 1.

The cranial end of the gland terminates in a blind bottom. An opening is noted in its caudal end, corresponding to the duct that discharges before the intestine and rectum junction, facilitating fluid elimination containing NaCl, isosmotic to plasma, through the digestive tract. The distance between the cranial and caudal ends of the rectal gland was of 3.6 centimeters, with a width of 1.2 centimeters (Fig. 2).

A microscopic analysis of the rectal gland indicated three main regions, namely the capsule, secretory parenchyma, and central duct (Fig. 3). Utilizing special trichromatic staining (Masson), the blood vessels comprising the gland's structure were visualized, with the tunica adventitia stained blue (Fig. 4). A small artery was discerned via trichromatic staining, highlighted by the presence of red-stained smooth muscle fibers. The superficial epithelium surrounding the capsule contains a layer of cuboidal cells, evident through basophilic staining using the Hematoxylin-eosin stain (Fig. 5). Lymphomyeloid tissue, containing myeloid cells indicative of extracellular hematopoiesis, was observed in the external capsule region (Fig. 6).

Composed of fibrous connective tissue and surrounded by a dense network of blood vessels, the capsule begins to fold inward as it approaches the secretory parenchyma, penetrating into the rectal gland and forming the interlobular septa (Fig. 7). Upon closer microscopic examination, fibroelastic tissue was observed between the secretory tubules, encasing them as a defining structure for each tubule, referred to as the intertubular septum (Fig. 8). Both the fibrous connective tissue of the capsule and the interlobular septa, as well as the fibroelastic tissue between the secretory tubules, were distinctly stained blue using trichromatic staining.

The interlobular septa were readily discernible in both staining methods, also allowing for the identification of an interlobular blood vessel (Fig. 9). Each interlobular septum divides the secretory parenchyma of the rectal gland into lobes containing multiple secretory tubules that converge towards the central duct.

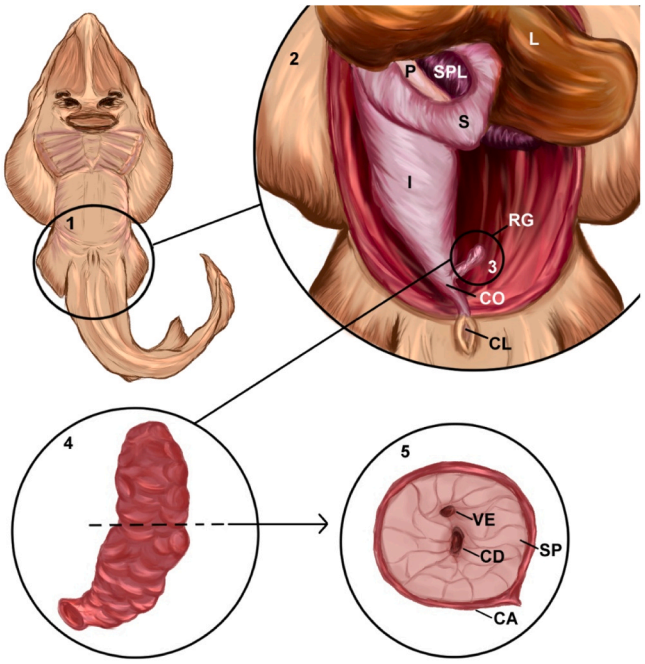

Fig. 1. Illustrative depiction of the anatomical location and macroscopic morphology of the rectal gland in *Pseudobatos horkelii*. The rectal gland (RG) resides within the caudal region of the animal's abdominal cavity (1). Accessing the abdominal cavity (2) and displacing the liver (L) facilitates identification of the rectal gland (3) positioned at the terminus of the post-valvular intestine (I), posterior to other organs within the cavity such as the stomach (S), pancreas (P), and spleen (SPL). The gland functions to expel excess salt absorbed by the animal into the colon (CO) and cloaca (CL) for elimination. Its lobulated surface (4) results from multiple secretory lobes, clearly discernible in cross-Section (5), where delineation of the connective tissue capsule (CA), secretory parenchyma (SP), central duct (CD), and venous blood vessel (VE) is evident. Source: Author compilation (2023). Adapted from Rutledge (2019); Melo et al. (2021); Suzer et al. (2022).

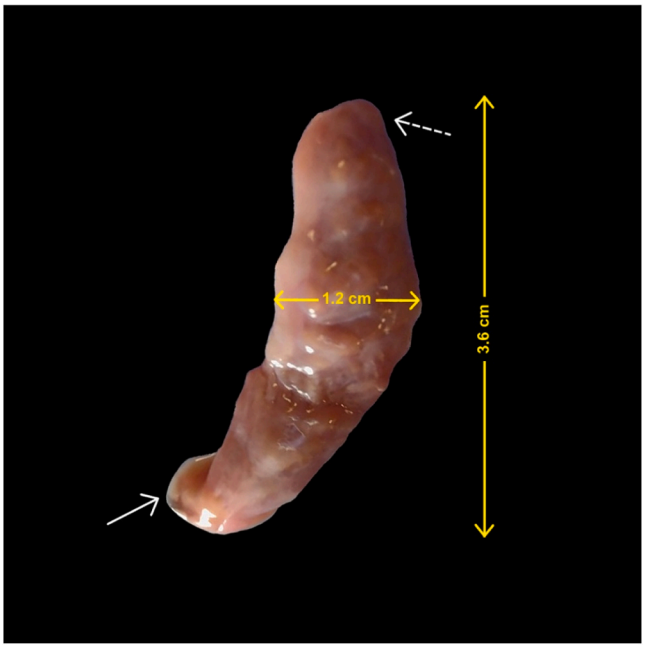

Fig. 2. Macroscopic appearance of the rectal gland in *Pseudobatos horkelii*, 1.2 centimeters in width and 3.6 centimeters in height. The gland's surface displays prominent lobulation, with the cranial termination (dashed white arrow) marking its blind termination, and the caudal termination (white arrow) indicating the opening into the post-valvular intestine.

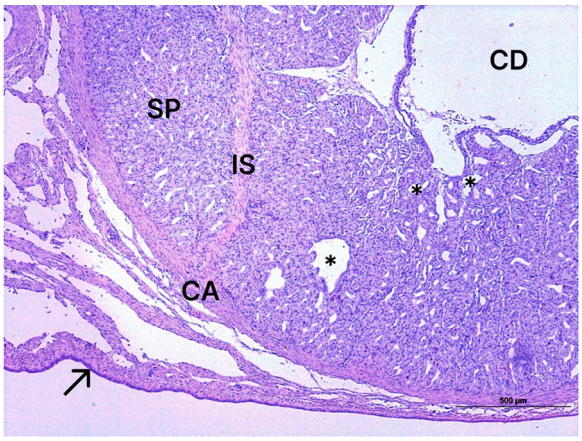

Fig. 3. Microscopic image a transverse section of the rectal gland in *Pseudobatos horkelii*, illustrating the capsule (CA), secretory parenchyma (SP), divided by the interlobular septum (IS), secretory tubules (asterisks), central duct (CD), and superficial epithelium (arrow). H/E stain.

A pattern was observed in the orientation and dimensions of the secretory tubules, characterized by larger luminal diameters and increased numbers of basophilic secretory cells in H/E staining as they approach the central duct, categorized as small, medium, and large (Fig. 10).

The central duct at the center of the rectal gland (Fig. 11a) functions as the conduit through which the secretory tubules from the entire secretory parenchyma of the organ discharge fluid. Its lumen is lined with pseudostratified epithelium, featuring acidophilic intraepithelial cells and mucous cells (Fig. 11b).

4. Discussion

The rectal gland of *Pseudobatos horkelii*, exhibits a digitiform morphology and modest dimensions, similar to that noted by Crofts (1925) for the bluntnose guitarfish *Rhinobatos blochii*. Rectal gland configuration, however, appears to vary among elasmobranch species. Notably, Ernst et al. (1981) described it as cylindrical in the Atlantic stingray *Dasyatis sabina,* now *Hypanus sabinus,* due to a taxonomic revision carried out in 2016), while Melo et al. (2021) reported an "S" shape in the longnose stingray *Hypanus guttatus* and the Brazilian large-eyed stingray *Hypanus mariane*. However, discrepancies in shape nomenclature also exist within studies on the same species. In the case of the spiny dogfish *Squalus acanthias*, Bulger (1965) described the rectal gland as a finger-shaped organ, whereas Ernst (1981) characterized it as cylindrical. Its digitiform structure arises from the characteristics of its lobulated surface, which, consequently, is influenced by a thin capsule and a small muscle layer enveloping the organ. This structural arrangement results in regions lacking lobular ducts, defining the gland's distinctive shape, similar to that reported by Melo et al. (2021) for *H. marianae*.

The rectal gland in *P. horkelii* is also characterized by a thin capsule and a small layer of smooth muscle, similar to *H. marianae* analyzed by Melo et al. (2021). The thin smooth muscle layer enveloping the rectal gland capsule is responsive to vasoactive stimuli, which regulates its contraction and relaxation, facilitating the excess salt secretion (Piermarini and Evans, 2000). In contrast, the spotted eagle ray *Aetobatus narinari* exhibits a thick muscle layer surrounding the capsule, which may be associated with habitat type or species phylogeny (Melo et al., 2021).

Lymphomyeloid tissue containing myeloid cells indicative of extracellular hematopoiesis was observed outside the capsule in *P. horkelii*,

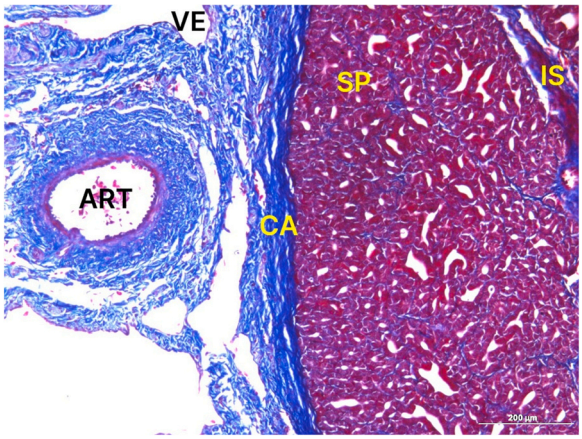

Fig. 4. Microscopy cross-section image of the rectal gland in *Pseudobatos horkelii* depicting the artery (ART) and venous blood vessel (VE) situated within the connective tissue forming the capsule (CA) and secretory parenchyma (SP), delineated by the interlobular septum (IS). Masson's Trichome stain.

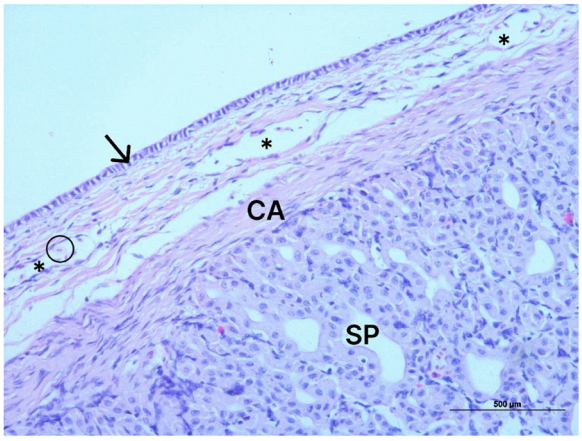

Fig. 5. Cross-sectional microscopy image of the rectal gland in *Pseudobatos horkelii*. The capsule (CA) encasing the secretory parenchyma (SP). Noticeable superficial epithelium consisting of a layer of cubic cells (arrow). Blood vessels (asterisks) containing red blood cells (circle) are evident within the capsule. H/E stain.

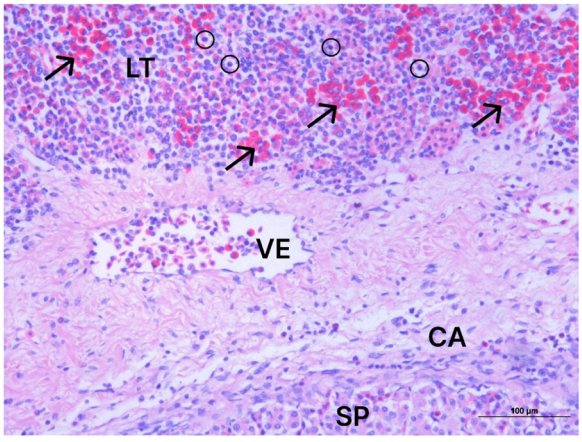

Fig. 6. Cross-sectional microscopy image of the rectal gland in *Pseudobatos horkelii*, depicting lymphomyeloid tissue (LT) containing lymphocytes (circles) and myeloid cells (arrows) surrounding the capsule (CA). A blood vessel (VE) is observed within the connective tissue of the capsule and secretory parenchyma (SP). H/E stain.

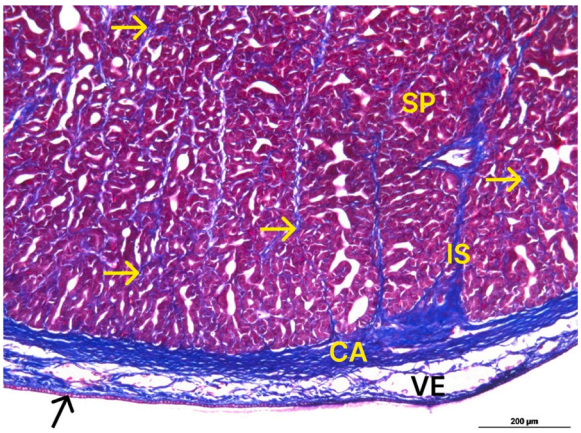

Fig. 7. Microscopy image of the rectal gland in *Pseudobatos horkelii,* revealing a distinct simple cuboidal superficial epithelium (black arrow), a capsule (CA) composed of fibrous connective tissue abundant in blood vessels (VE), an interlobular septum (IS) formed by the infolding of the capsule into the secretory parenchyma, and fibroelastic tissue (yellow arrow) surrounding the secretory tubules. Masson's Trichrome stain.

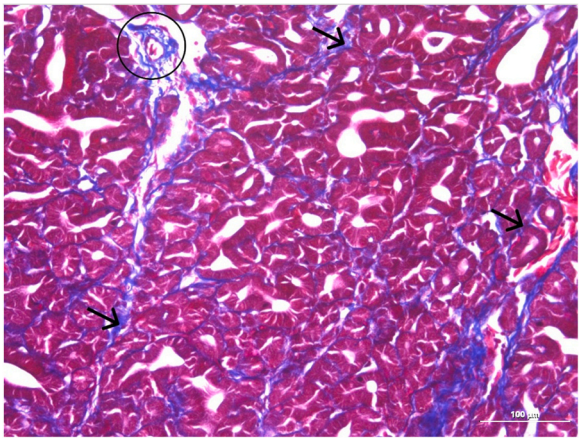

Fig. 8. Microscopy image of the rectal gland in *Pseudobatos horkelii,* illustrating the secretory parenchyma at higher magnification, with secretory tubules surrounded by fibroelastic tissue (arrows) and an interlobular blood vessel (circle). Masson's Trichrome stain.

similar to *A. narinari* (Melo et al., 2021) and *R. blochi* (Crofts, 1925). Melo et al. (2021) also report that the longnose stingray *H. guttatus*, a euryhaline species, *i.e.*, able to tolerate wide salinity ranges, exhibited acidophilic cells within the stratified epithelium of the central duct, similar to that observed in *H. sabinus* (Piermarini and Evans, 2000), and the *P. horkelii* analyzed herein. According to Dezfuli et al., 2018), the function of these acidophilic cells is likely associated to primary intestinal defense mechanisms. although further research is required to fully elucidate their role within the rectal gland (Melo et al., 2021).

The central duct epithelium in *P. horkelii* appears pseudostratified, with no regular cuboidal cell layering. This contrasts with the findings of Ernst et al. (1981) and Bulger (1965), who described the epithelium of the central duct as stratified. Bulger (1965), in contrast, compared the ultrastructural characteristics of the central duct epithelium to those of the amphibian urinary bladder, noting their shared ultrastructural features. The pseudostratified epithelium in *P. horkelii* consists of 4–8 cells, in agreement with the initial study of Ernst et al. (1981). The surface of the epithelium of the central duct consists of specialized cells, classified into four distinct types by Bulger (1965): granular cells, mucous cells, flask-shaped cells, and cells with large mitochondria. Most cells in the luminal layer of the central duct in *P. horkelii* are similar to the granular

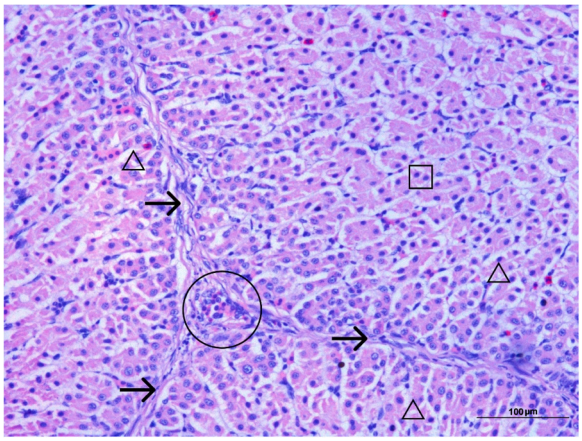

Fig. 9. Microscopy image of the rectal gland in *Pseudobatos horkelii*, revealing a delicate interlobular septum (arrows) dividing three secretory lobes comprising numerous secretory tubules. Basophilic secretory cells (square), interlobular blood vessel (circle), and cytoplasmic vacuoles (triangles) are observerd within the tubular epithelium. H/E stain.

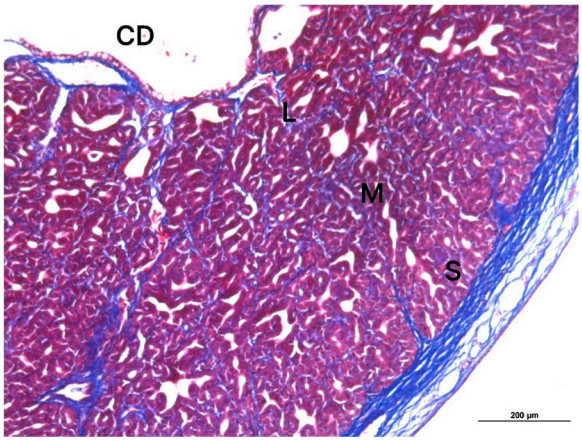

Fig. 10. Microscopy image of the secretory parenchyma of the rectal gland in *Pseudobatos horkelii*, featuring small (S), medium (M), and large (L) tubules along with the central duct (CD). Masson's Trichrome stain.

cells found in the amphibian urinary bladder, as observed by Ernst et al. (1981) in the spiny dogfish *Squalus acanthias*, by Bulger (1965) in the Pacific spiny dogfish *Squalus suckleyi* and by Melo et al. (2021) in *H. marianae.*

The mucous cells described by Bulger (1965) are likewise observed in the central duct of *P. horkelii*. However, while Bulger (1965) reported a higher abundance of these cells near the glandular duct, in the present study, they are observed exclusively in the vicinity of the central duct. The differentiation between flask-shaped cells, cells containing large mitochondria and cells located in the intermediate and basal region of the central duct was not possible, as it would require higher magnification in the microscopy analyses.

The secretory parenchyma of *P. horkelii* is composed of simple and branched secretory tubules lined with a simple columnar epithelium. These tubules radiate from the central duct and end blindly against an external fibromuscular capsule, creating a convoluted cytoarchitecture when observed in cross-section, these findings are consistent with those reported by Ernst et al. (1981) in the spiny dogfish, *Squalus acanthias*. The secretory tubules vary in size - small, medium, and large - and demonstrate an increase in the number of secretory cells as well as an enlargement of their luminal diameter as they approach the central duct, similar to that reported by Melo et al. (2021) for *H. guttatus* and

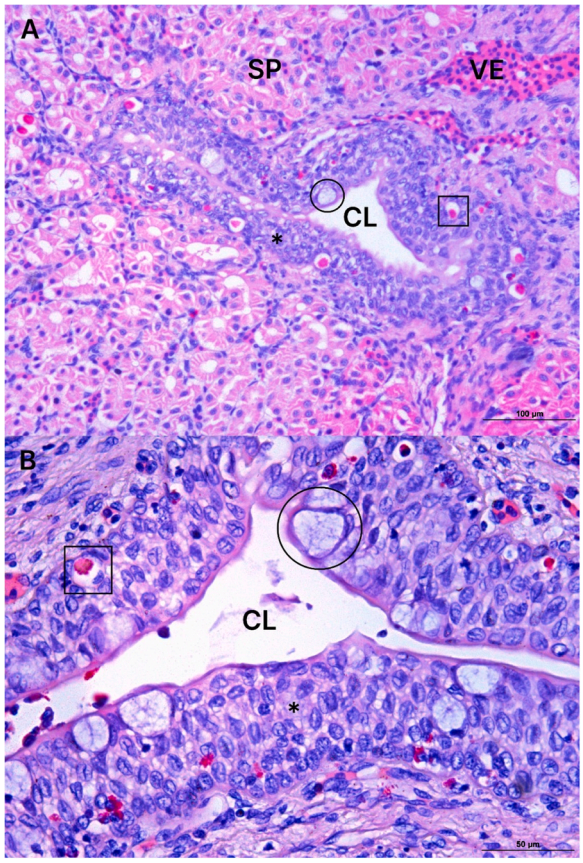

Fig. 11. Microscopy image of the rectal gland in *Pseudobatos horkelii*. A – Cross-section of the central lumen (CL) lined with pseudostratified epithelium (asterisk), acidophilic intraepithelial cells (square), and mucous cells (circle). A blood vessel (VE) is located within *the secretory parenchyma (SP). H/E stain. B – Higher magnification view of the central duct lumen of the rectal gland in cross-section, showing pseudostratified epithelium (asterisk*), acidophilic intraepithelial cells (square), and mucous cells (circle). H/E stain.

A. narinari. Lumen dilation near the central duct is attributed to an increased surface area required for salt secretion, while the specialized epithelium of the central duct likely functions to maintain the balance of its contents with systemic fluids (Newbound and O'Shea, 2001).

The findings reported herein are similar to those reported by Melo et al. (2021) regarding *H. guttatus*, a ray capable of transitioning between saltwater and brackish water habitats (Thorson and Brooks., 1983) that engages in benthic feeding, similar to *P. horkelii* (McEachran and Carvalho, 1999). This adaptive behavior requires the ability to rapidly modulate NaCl secretion in the rectal gland in response to varying environmental salinities, a trait also observed in the euryhaline stingray *H. sabinus* (Piermarini and Evans, 1998; Piermarini and Evans, 2000), as well as in *H. guttatus* (Melo et al., 2021) and notably in *P. horkelii* as evidenced herein.

In this sense, cytoplasmic vacuoles in the secretory cells of rectal glands are associated with low secretory activity or fasting (Chan and Phillips, 1967). In this sense, Melo et al. (2021) proposed that morphological rectal gland changes are influenced not only by environmental salinity but also significantly by diet, although these authors also suggest that vacuolated cytoplasm in the secretory cells of *H. guttatus* likely results from habitat preference for brackish water rather than feeding challenges. Given that *P. horkelii* shares similar benthic habitat and feeding characteristics, occupying a mesotrophic position (Bornatowski et al., 2010; Stevens et al., 2000), the occurrence of cytoplasmic vacuoles in rectal gland secretory cells may potentially be attributed to its ability to tolerate brackish water. In the present study,

however, few cytoplasmic vacuoles were observed in the rectal gland of the *P. horkelii* individual analyzed herein, possibly due to the fact that the specimen was captured in an oceanic environment, and not brackish.

Most findings reported herein align with those observed in other euryhaline species inhabiting benthic-demersal habitats and engaging in benthic feeding. Although morphological rectal gland distinctions among species are subtle, they become particularly noticeable when compared with freshwater and saltwater species due to the direct influence of environmental salinity on the functionality of osmoregulatory organs. Given that the *Pseudobatos* genus comprises euryhaline species, the rectal gland of *P. horkelii* exhibits macroscopic and microscopic features indicative of heightened functionality, closely associated to the species' capacity to transition between brackish and saline waters while foraging in benthic-demersal environments.

This study represents the first comprehensive investigation to conduct a morphological analysis encompassing both macroscopic and microscopic rectal gland aspects in *P. horkelii.* Most morphological features align with those documented in prior studies involving other rays sharing similar phylogeny, habitat, and feeding characteristics compared to *P. horkelii.* The findings regarding secretory parenchyma cytoplasmic vacuoles, the presence of numerous acidophilic cells in the stratified central duct epithelium, and the enlargement of the secretory tubule lumens near the central duct provide insights into the behavioral adaptations of this species concerning osmoregulation. Additionally, the evident lobulation observed macroscopically on the organ's surface indicates high functional rectal gland capacity.

The contribution of this histological rectal gland assessment in *P. horkelii* is particularly valuable given the species highly endangered status, facilitates pathological assessments in highly contaminated environments that may compromise this species resilience.

CRediT authorship contribution statement

Queiroz de Carvalho Eulógio Carlos: Writing – review & editing, Writing – original draft, Supervision, Resources, Data curation. **Hauser-Davis Rachel Ann:** Writing – review & editing, Supervision, Resources, Project administration, Funding acquisition, Data curation, Conceptualization. **Jerdy Hassan:** Writing – original draft, Investigation, Formal analysis, Data curation. **França Lopes Beatriz:** Writing – review & editing, Writing – original draft, Visualization, Methodology, Investigation, Formal analysis, Data curation. **Vieira Gomes Géssica:** Writing – original draft, Investigation, Formal analysis, Data curation.

Declaration of Competing Interest

The authors declare no conflict of interest.

Acknowledgements

Thanks are due to Aline de Oliveira Felix, Renata Morais Silva and Patrick Gabriel Alencar dos Santos for their assistance during the preparation and investigation of the original draft of this research. RAHD would like to thank the Carlos Chagas Filho Foundation for Research Support of the State of Rio de Janeiro (FAPERJ) through grant numbers E-26/210.300/20222 (Apoio ao Jovem Pesquisador Fluminense com Vínculo em ICTS do Estado do RJ 2021), E-26/201.270/202 (Jovem Cientista do Nosso Estado 2021–2024) and the Brazilian National Council of Scientific and Technological Development (productivity grant, process number 308811/2021–6). The implementation of the Projeto Pesquisa Marinha e Pesqueira is a compensatory measure established by the Conduct Adjustment Agreement under the responsibility of the PRIO company, conducted by the Federal Public Ministry – MPF/RJ.

Data availability

Data will be made available on request.

References

Amaral, C.R.L., Pereira, F., Silva, D.A., Amorim, A., de Carvalho, E.F., 2017. The mitogenomic phylogeny of the Elasmobranchii (Chondrichthyes). Mitochondrial DNA Part A 29 (6), 867–878.

Aschliman, N.C., Nishida, M., Miya, M., Inoue, J.G., Rosana, K.M., Naylor, G.J.P., 2012. Body plan convergence in the evolution of skates and rays (Chondrichthyes: Batoidea). Mol. Phylogenetics Evol. 63 (1), 28–42. https://doi.org/10.1016/j.ympev.2011.12.012.

Bornatowski, H., Robert, M., Costa, L., 2010. Feeding of guitarfish *Rhinobatos percellens* (Walbaum, 1972) (Elasmobranchii, Rhinobatidae), the target of artisanal fishery in southern Brazil. Braz. J. Oceano 58 (8), 45–52. https://doi.org/10.1590/s1679-87592010000100005.

Boylan, J., Feldman, B., Antowiak, D., 1967. Gills permeability in *Squalus acanthias*. In: Gilbert, P., Mathewson, R., Rall, D. (Eds.), Shark, skates and rays. Johns Hopkins Press, pp. 197–206.

Bulger, R.E., 1965. Electron microscopy of the stratified epithelium lining the excretory canal of the dogfish rectal gland. Anat. Rec. 151, 589–607. https://doi.org/10.1002/ar.1091510410.

Burger, J., Hess, W., 1960. Function of the rectal gland in the spiny dogfish. Science 131 (3401), 670–671. https://doi.org/10.1126/science.131.3401.670.

Chan, D., Phillips, J., 1967. The anatomy, histology and histochemistry of the rectal gland in lip-shark Hemiscylium plagiosum (Bennet). J. Anat. 101 (21), 137–157.

Chenhong, L., Matthes-Rosana, K.A., Garcia, M., Naylor, G.J.P., 2012. Phylogenetics of Chondrichthyes and the problem of rooting phylogenies with distant outgroups. Mol. Phylogenetics Evol. 63 (2), 365–373.

Crofts, D., 1925. The comparative morphology of the caecal gland (rectal gland) of selachian fishes, with some reference to the morphology and physiology of the similar intestinal appendage throughout Ichthyopsida and Sauropsida. Zool. Soc. Lond. 95, 101–188. https://doi.org/10.1111/j.1096-3642.1925.tb03346.x.

Dantzler, W., 1989. Comparative Physiology of the Vertebrate kidney. APS (292), 11–87. https://doi.org/10.1002/cphy.cp080111.

Dezfuli, S., Manera, M., Bosi, G., Merella, P., Depasquale, J., Giari, L., 2018. Description of epithelial granular cell in catshark spiral intestine: Immunohistochemistry and ultrastructure. J. Morphol. 280 (9), 205–213. https://doi.org/10.1002/jmor.20932.

Doyle, W., 1962. Tubule cells of the rectal salt gland of Urolophus. Am. J. Anat. 111 (15), 223–237. https://doi.org/10.1002/aja.1001110208.

Dulvy, N.K., Pacoureau, N., Rigby, C.L., Hilton-Taylor, C., Fordham, S.V., Simpfendorfer, C.A., 2021. Overfishing drives over one-third of all sharks and rays toward a global extinction crisis. Curr. Biol. 31, 4773–4787. https://doi.org/10.1016/j.cub.2021.08.062.

Erlij, D., Rubio, J., 1986. Control of rectal gland secretion in the dogfish (*Squalus acanthias*): Steps in the sequence of activation. J. Exp. Biol. 122 (1), 99–112. https://doi.org/10.1242/jeb.122.1.99.

Ernst, S.A., Hootman, S.R., Schreiber, J.H., Riddle, C.V., 1981. Freeze-fracture and morphometric analysis of occluding junctions in rectal glands of elasmobranch fish. J. Membr. Biol. 58 (2), 101–114. https://doi.org/10.1007/BF01870973.

Eyckmans, M., Lardon, I., Wood, C.M., De Boeck, G., 2013. Physiological effects of waterborne lead exposure in spiny dogfish (*Squalus acanthias*). Aquat. Toxicol. 126, 373–381. https://doi.org/10.1016/j.aquatox.2012.09.004.

Fricke, R., Eschmeyer, W.N., & Van der Laan, R. (2024). Eschmeyer's catalog of fishes: Genera, Species, References. Retrieved October 2, 2022, from ⟨http://researcharchive.calacademy.org/research/ichthyology/catalog/fishcatmain.asp⟩.

Leibold, M.A., Holyoak, M., Mouquet, N., Amarasekare, P., Chase, J.M., Hoopes, M.F., et al., 2004. The metacommunity concept: A framework for multi-scale community ecology. Ecol. Lett. 7 (7), 601–613. https://doi.org/10.1111/j.1461-0248.2004.00608.x.

Leite, R.D., Wosnick, N., Lopes, A.P., Dillenburg Saint'Pierre, T., Vianna, M., Hauser-Davis, R.A., 2023. Ecotoxicology applied to conservation: Potential negative metal and metalloid contamination effects on the homeostatic balance of the critically endangered Brazilian guitarfish, *Pseudobatos horkelii* (Elasmobranchii: Rhinobatidae). Chemosphere 341, 140119. https://doi.org/10.1016/j.chemosphere.2023.140119.

Lessa, R., Vooren, C.M., Lahayne, J., 1986. Desenvolvimento e ciclo sexual das fêmeas, migrações e fecundidade da viola Rhinobatos horkelii (Muller & Henle, 1841) do sul do Brasil. Atlantica 8 (1), 5–34.

Lund, R., Grogan, E.D., 1997. Relationships of the Chimaeriformes and the basal radiation of the Chondrichthyes. Rev. Fish. Biol. Fish. 7 (1), 65–123. https://doi.org/10.1023/A:1018471324332.

Martins, R.R., Schwingel, P.R., 2003. Variação espaço-temporal da CPUE para o gênero *Rhinobatos* (Rajiformes, Rhinobatidae) na costa sudeste e sul do Brasil. Notas Técnicas FACIMAR 7, 119–129. https://doi.org/10.14210/bjast.v7n1.p119-129.

McEachran, J.D., Carvalho, M.R., 1999. Batoids. In: Carpenter, K.E., Niem, V.H. (Eds.), The living marine resources of the Western Central Pacific. Vol. 3. Batoid fishes, chimaeras and bony fishes, Part 1. Elopidae to Linophrynidae. FAO Species Identification Guide for Fishery Purposes, Rome, pp. 507–589.

Melo, A.C.M., Andrade, C.B., Poscal, A., Rêgo, M.G., Sá, F.B., Neto, J., Araújo, M.L.G., 2021. Ecomorphology of the rectal gland of three batoids (Elasmobranchii: Myliobatiformes). Zool. Anz. 293 (8), 225–232. https://doi.org/10.1016/j.jcz.2021.06.010.

Newbound, D.R., O'Shea, J.E., 2001. The microanatomy of the rectal gland of the Port Jackson shark, *Heterodontus portusjacksoni* (Meyer) (Heterodontidae): Suggestions for a counter-current exchange system. Cells Tissues Organs 169 (11), 165–175. https://doi.org/10.1159/000047875.

Nishida, K., 1990. Phylogeny of the suborder Myliobatidoidei. Mem. Fac. Fish. Hokkaido Univ. 37 (109), 1–108.

Piermarini, P.M., Evans, D.H., 1998. Osmoregulation of the Atlantic stingray (*Dasyatis sabina*) from the freshwater lake Jesup of the St. Johns River, Florida. Physiol. Zool. 71 (9), 553–560. https://doi.org/10.1086/515973.

Piermarini, P.M., Evans, D.H., 2000. Effects of environmental salinity on Na (+)/K (+)-ATPase in the gills and rectal gland of a euryhaline elasmobranch (*Dasyatis sabina*). J. Exp. Biol. 203 (10), 2957–2966. https://doi.org/10.1242/jeb.203.19.2957.

Rutledge, K.M., 2019. A new guitarfish of the genus Pseudobatos (Batoidea: Rhinobatidae) with key to the guitarfishes of the Gulf of California. Copeia 107 (13), 454–457. https://doi.org/10.1643/CI-18-166.

Silva, P., Evans, D.H., 2024. The rectal gland of the shark: The road to understanding the mechanism and regulation of transepithelial chloride transport. Kidney 360 5 (3), 471–480.

Stevens, J.D., Bonfil, R., Dulvy, N.K., Walker, P.A., 2000. The effects of fishing on sharks, rays, and chimaeras (Chondrichthyans), and the implications for marine ecosystems. ICES J. Mar. Sci. 57, 476–494. https://doi.org/10.1006/jmsc.2000.0724.

Solomon, J.T., Taylor, L.E., Wilkins, R.G., 1985. Primary role of volume expansion in stimulation of rectal gland function. Am. J. Physiol. - Regul., Integr. Comp. Physiol. 248, R638–R640.

Solomon, J.T., Taylor, L.E., Wilkins, R.G., 1984. In vivo effect of volume expansion on rectal gland function. I. Humoral factors. Am. J. Physiol. 246, R63–R66. https://doi.org/10.1152/ajpregu.1984.246.1.R63.

Suzer, B., Yalgin, F., Saticioglu, I.B., Taskin, M., Yavas, O., Duman, D., 2022. Macroscopic examination of cownose rays (*Rhinoptera bonasus*). J. Anatol. Env Anim. Sci. 7 (4), 446–458. https://doi.org/10.35229/jaes.1177624.

Thorson, T.B., Brooks, D.R., 1983. The evolution of freshwater adaptation in stingrays. Nat. Geog Soc. Res Rep. 15, 663–694.

Vooren, C.M., Lessa, R., Klippel, S., 2005. Biologia e status de conservação da viola *Rhinobatos horkelii*. In: Vooren, In.C.M., Klippel, S. (Eds.), Ações para a conservação de tubarões e raias no Sul do Brasil. Porto Alegre: Igaré, p. 246.

Wosnick, N., Niella, Y., Hammerschlag, N., Chaves, A.P., Hauser-Davis, R.A., Chávez da Rocha, R.C., Jorge, M.B., Santos de Oliveira, R.W., Nunes, J.L.S., 2021. Negative metal bioaccumulation impacts on systemic shark health and homeostatic balance. Mar. Pollut. Bull. 168, 112398. https://doi.org/10.1016/j.marpolbul.2021.112398.